applied sciences

MDPI

Article

Surface Texture Measurement on Complex Geometry Using Dual-Scan Positioning Strategy

Fang Cheng [1], Shaowei Fu [2,3,*] and Ziran Chen [1]

[1] Engineering Research Center of Mechanical Testing Technology and Equipment (Ministry of Education), Chongqing Key Laboratory of Time Grating Sensing and Advanced Testing Technology, Chongqing University of Technology, Chongqing 400054, China; chf19chf19@hotmail.com (F.C.); czr@cqut.edu.cn (Z.C.)

[2] School of Mechanical and Aerospace Engineering, Nanyang Technological University, Singapore 639798, Singapore

[3] JM VisTec System Pte Ltd., Singapore 417942, Singapore

* Correspondence: FUSH0009@e.ntu.edu.sg

Received: 3 November 2020; Accepted: 24 November 2020; Published: 26 November 2020

check for updates

Featured Application: This work is potentially applicable to in-line surface measurement. Integrated with robots or other manipulation devices, the proposed technology will be able to capture surface finishing parameters, including roughness and surface texture uniformity.

Abstract: In this paper, a surface measurement method based on dual-scan positioning strategy is presented to address the challenges of irregular surface patterns and complex geometries. A confocal sensor with an internal scanning mechanism was used in this study. By synchronizing the local scan, enabled by the internal actuator in the confocal sensor, and the global scans, enabled by external positioners, the developed system was able to perform noncontact line scan and area scan. Thus, this system was able to measure both surface roughness and surface uniformity. Unlike laboratory surface measurement equipment, the proposed system is reconfigurable for in situ measurement and able to scan free-form surfaces with a proper stand-off distance and approaching angle. For long-travel line scan, which is needed for rough surfaces, a surface form tracing algorithm was developed to ensure that the data were always captured within the sensing range of the confocal sensor. It was experimentally verified that in a scanning length of 100 mm, where the surface fluctuation in vertical direction is around 10 mm, the system was able to perform accurate surface measurement. For area scan, XY coordinates provided by the lateral positioning system and the Z coordinate captured by the confocal sensor were plotted into one coordinate system for 3D reconstruction. A coherence scanning interferometer and a confocal microscope were employed as the reference measurement systems to verify the performance of the proposed system in a scanning area of 1 mm by 1 mm. Experimental data showed that the proposed system was able to achieve comparable accuracy with laboratory systems. The measurement deviation was within 0.1 µm. Because line scan mechanisms are widely used in sensor design, the presented work can be generalized to expand the applications of line scan sensors.

Keywords: surface texture measurement; confocal sensing; surface form tracing; 3D reconstruction; roughness

1. Introduction

An important tool for product quality assessment, surface texture measurements are traditionally performed based on laboratory systems, due to the high degree of measurement resolution required [1,2].

With the rapid development of advanced manufacturing technologies, such as five-axis machining and additive manufacturing (AM), new surface measurement solutions are needed to address the challenges of complex geometries and irregular surface patterns [3,4]. Stylus profilometry is widely used for conventionally machined samples [5]. Equipped with a coordinate measuring machine (CMM), the measurement space of stylus profilometry can be enlarged to accommodate samples of large volume and complicated geometry [6]. However, stylus profilometry is not an ideal solution for measuring surfaces with irregular patterns due to its contact measurement mechanism and flanking errors [7,8]. Another limitation of stylus profilometry is its low efficiency for areal surface texture measurement. Therefore, based on ISO 4287 [9], stylus profilometry is mainly used in line scan mode for conventionally machined surfaces with known directional surface patterns. 3D microscopy [10], such as confocal microscopy [11–13], coherence scanning interferometry [14,15] and focus variation microscopy [16,17], are suitable for area scans. 3D microscopic systems are able to determine surface roughness and surface isotropy based on ISO 25178-2 [18,19]. Using objectives with high numerical aperture (NA), 3D microscopic systems are able to achieve much higher lateral resolution compared with stylus profilometry. However, the vertical measurement range relies on mechanical scanning, which significantly limits measurement efficiency. In order to avoid mechanical movement, the concept of chromatic confocal microscopy (CCM) [20,21] has been developed in the past decade. However, for high-accuracy measurement, CCM's sensing range is within a few hundreds of microns, which limits its application to free-form surface measurement. Furthermore, when measuring high-roughness surfaces, long scans are required to differentiate surface roughness from surface waviness and surface form [22]. Therefore, a large vertical measurement range is needed to cover surface fluctuations over a long scan range.

Based on the above literature review and analysis, the motivation of this presented work is to develop an optical surface texture measurement system able to perform both line and area scans for challenging surfaces with complex geometry and irregular surface patterns. Unlike a laboratory solution, the proposed system has the potential to be utilized for in situ measurement [23,24].

2. Principle of Confocal Sensing with Internal Scanning

A laser confocal sensor, Keyence LT9011 (KEYENCE, Osaka, Japan), was utilized for surface height measurement in this study. Figure 1a shows the general principle of a single-point confocal sensor. Only when the measurement point is in focus will the detector receive the peak intensity of the reflected laser. Figure 1b shows the working principle of the Keyence LT9011. The optics are driven by a tuning fork to generate high-frequency vibration, enabling vertical scanning. In the meantime, the focus position can be detected and height can be measured accordingly. The optics are also driven by an oscillating unit for lateral scanning, with a frame rate of 2.8 fps covering a scan length of 1.1 mm. This product was originally developed for height or thickness measurements.

The vertical resolution of the LT9011 is 0.1 µm. The laser beam spot size is 2 µm with a scanning spacing of 2 µm, which complies with the requirements for surface roughness measurements based on ISO 4287 [9]. In this study, this sensor was further developed for surface texture measurement.

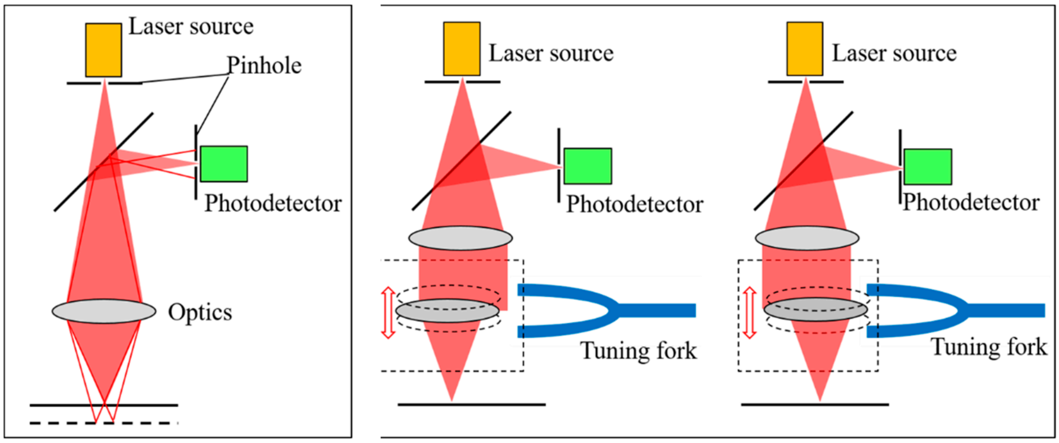

(**a**) (**b**)

Figure 1. Principle of confocal sensing with internal scanning: (**a**) principle of confocal sensor; (**b**) internal scanning mechanism.

With the internal scanning mechanism, this sensor is able to measure surface roughness subject to two conditions:

(1) the surface is relatively flat; the surface fluctuation does not exceed the sensing range of 0.6 mm;
(2) the surface is relatively smooth; the measurement of roughness parameters does not require a roughness evaluation length longer than 1.1 mm.

Figure 2 shows the measured surface profile of a calibrated roughness master (178–602, Mitutoyo Corporation, Kawasaki-shi, Japan) with known *Ra* and *Rt* values of 2.97 µm and 9.4 µm, respectively.

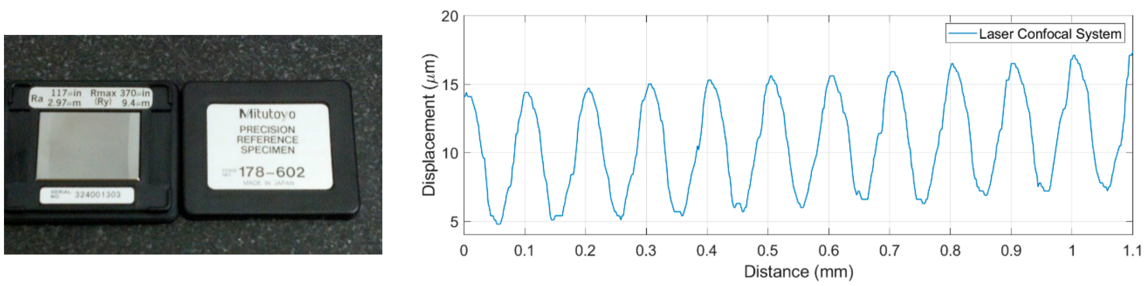

Figure 2. Line scan for roughness measurement using confocal sensing.

The arithmetical mean roughness (*Ra*) can be calculated using Equation (1), where N is the number of data points acquired in a measurement and Z_i is the ith data point in height direction of the roughness profile. The total height of roughness profile (*Rt*) is defined as the difference between the largest profile peak height and the largest profile valley depth within the evaluation length [9].

$$R_a = \frac{1}{N}\sum_{i=1}^{N}|Z_i|. \quad (1)$$

Therefore, with Z_i values captured by the confocal sensor LT9011, the surface roughness parameter *Ra* over a scan length of 1.1 mm can be calculated. To verify the measurement capability of the laser confocal sensor LT9011, measurement results of the roughness master are shown in Table 1. The nominal *Ra* and *Rt* values of the roughness master are 2.97 µm and 9.40 µm, respectively. The mean error and standard deviation are 0.06 µm and 0.04 µm for *Ra* measurements and 0.10 µm and 0.08 µm for *Rt* measurements. The measurement error is partially due to short sampling length.

Table 1. Roughness master measurement result (unit: µm).

	1	2	3	4	5	Mean	Std. Dev.
***Ra* (µm)**	3.02	3.02	3.10	3.00	3.01	3.03	0.04
***Rt* (µm)**	9.51	9.43	9.67	9.46	9.48	9.50	0.08

3. 3D Surface Topography Measurement with Dual-Scan Scanning

Integrated with an external motorized stage (PT1/M-Z8, Thorlabs Inc., Newton, NJ, USA), a 3D surface topography measurement system was configured, as shown in Figure 3a. By synchronizing the internal and external scan, the 3D surface topography of the measured area was reconstructed, as shown in Figure 3b. The scanning area was 1.1 mm by 1 mm, with point spacing and line spacing of 2 µm. The total measurement time was 250 s.

The motivation for developing this system was to address the challenge of measuring geometrically complicated samples. Instead of accommodating the sample into the measurement space of a laboratory system, the measurement system was designed to approach the samples for adaptive measurement.

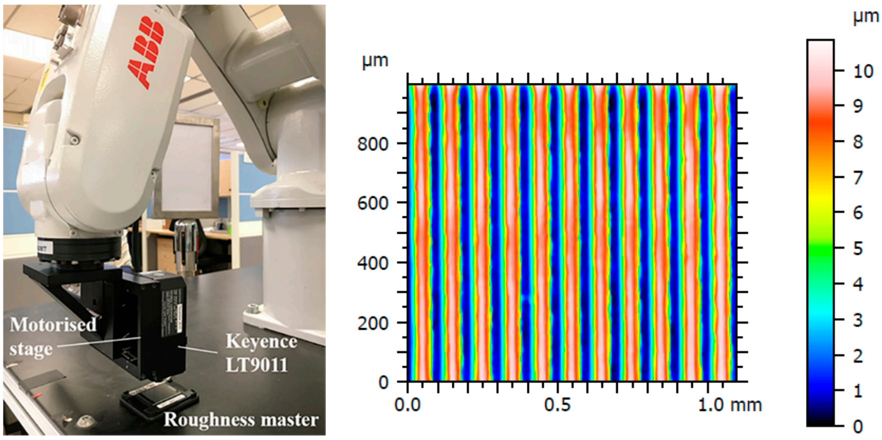

(**a**) (**b**)

Figure 3. 3D surface topography measurement based on confocal sensing: (**a**) system configuration; (**b**) 3D surface topography.

Based on the captured 3D surface topography, surface texture parameters were calculated as follows:

(1) height parameters Sa and Sq, for general understanding of the surface roughness;
(2) statistic parameters Ssk and Sku, to evaluate the dominant feature of the surface, peak dominant or valley dominant, as reference for further surface finishing process;
(3) spatial parameters Str and Std, to characterize the uniformity and analyze the directional patterns of the surface texture, if any.

Section 5.1 will provide the experimental data to verify the measurement performance.

4. Surface Tracing Strategy for Long Scan Length

In order to expand both the lateral and vertical measurement ranges of the line scan sensor, a dual-scan surface tracing algorithm was developed in this study. For rough surfaces, a long scanning length is needed to separate the information of roughness, waviness and form. Based on ISO 4288, for example, if the *Ra* value is greater than 10 µm, the cut-off length is recommended to be 8 mm, and five cut-offs are recommended for averaging computations. The entire scanning length would be 40 mm. For a free-form surface, the profile over such a scan length is very likely to exceed the vertical sensing range of a laser confocal sensor. In this study, therefore, a surface tracing control algorithm was developed to extend the vertical measurement range.

4.1. Surface Tracing Algorithm

For high-resolution surface measurement, the confocal sensing range in the vertical direction is typically less than 1 mm. The Keyence LT9011 laser confocal sensor used in this study has a vertical sensing range of 0.6 mm. When measuring rough surfaces with significant curvature, the measurement is very likely to fail due to insufficient sensing range, as shown in Figure 4a. In order to ensure surface information was always captured within the sensing range, an adaptive surface tracing algorithm was developed.

The methodology is illustrated in Figure 4b. The sensor moved in piece-wise mode. Each unit travel length was 1 mm. Since the oscillating unit inside the senor was able to generate a local scan length of 1.1 mm, the scanning range of the neighboring scans had an overlapping section of 0.1 mm. This overlapping section was used for profile reconstruction based on the best fitting algorithm [25].

In this system, a vertical positioner (LS-110, Physik Instrumente GmbH & Co. KG, Karlsruhe, Germany) was used to position the sensor to ensure that at each lateral scanning location, the data capture was within the sensing range. The positioner LS-110 was able to achieve a maximum speed of 90 mm/s and a positioning resolution of 50 nm in a range of 26 mm. The actual speed needed in this study depends on the lateral movement speed and the height variation of the measured surface. Since the lateral scanning speed generated by the internal positioner was 2 mm/s, this vertical positioner LS-110 had sufficient capability for most use cases.

At each location, the sensor LT9011 collected height information over a scan length of 1.1 mm. With the lateral position information determined by the sampling spacing and sequence number, a second-order polynomial $f(x)$ was obtained based on least-squares fitting. Then, the height to position the sensor for the next scan was determined as

$$h_{j+1} = \frac{1}{2}f'(x_n) + f(x_n). \tag{2}$$

where $f'(x)$ is the first derivate of $f(x)$, l is the lateral positioning increment and n is the number of data points acquired in l. In this study, l and n were set as 1.1 mm and 551, respectively.

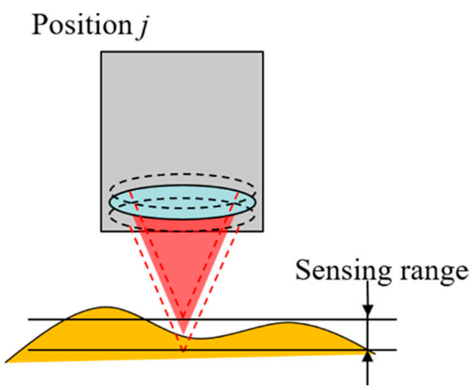

(a)

Figure 4. *Cont.*

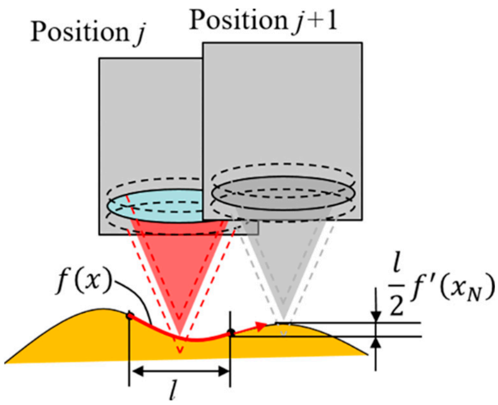

(**b**)

Figure 4. Surface tracing strategy to extend the measurement range: (**a**) measurement out of sensing range; (**b**) surface tracing.

The vertical positioner has an embedded optical encoder to record the position. Therefore, the height $z_{i,j}$ measured by the system included two portions: the height measured by the senor LT9011 and the height read from the optical encoder.

Figure 5a shows the setup for measuring a free-form surface. The sample was carried by a linear stage (TSA100-B, Zolix Instruments Co., Ltd., Beijing, China), the displacement of which was measured by an in-house developed image grating system [26,27]. Using this integrated system, the scanning range can be expanded to 100 mm. In this study, at each location, time taken for positioning and local scan was 1 s.

Figure 5b shows the scanning result. The vertical measurement range can be expanded using the proposed surface tracing algorithm.

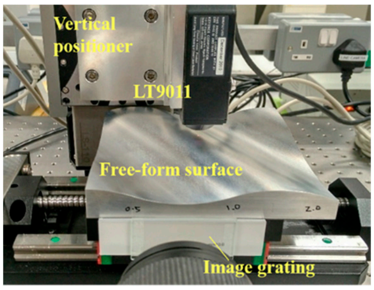

(**a**)

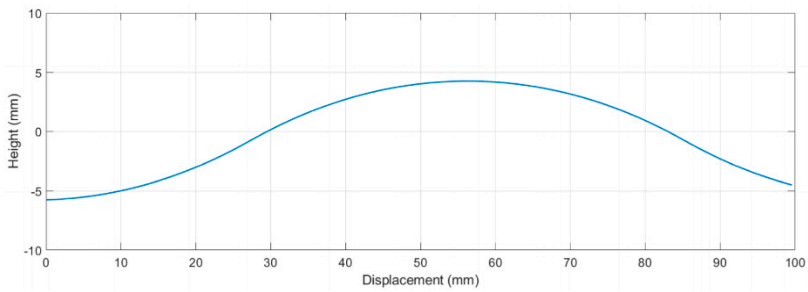

(**b**)

Figure 5. Free-form surface measurement: (**a**) system configuration; (**b**) scan data.

4.2. Correction of Misalignment

The misalignment of the internal and external scan needed to be calibrated. Instead of physically parallelizing the two moving axes, a pre-test on an optical flat (Figure 6a) was conducted to determine the misalignment. With the data collected from all sections plotted into one coordinate system, the measured profile is illustrated in Figure 6b.

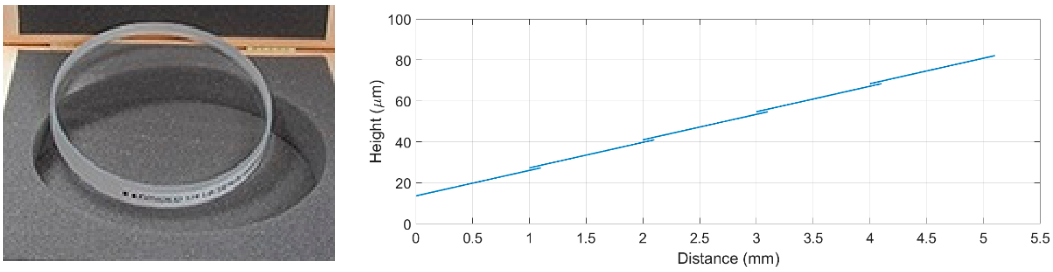

(**a**) (**b**)

Figure 6. Profile data misalignment illustration: (**a**) optical flat; (**b**) measured surface profile.

Discontinuity between neighboring sections can be corrected by introducing a vertical shift Δd to compensate for the misalignment. The corrected height values can be expressed as

$$\begin{cases} z'_{i,0} = z_{i,0} + 0; \\ z'_{i,1} = z_{i,1} + \Delta d; \\ z'_{i,2} = z_{i,2} + 2\Delta d; \\ \quad \cdots \\ z'_{i,m-1} = z_{i,m-1} + m\Delta d. \end{cases} \tag{3}$$

where m is the number of data sections. These equations can be generalized as

$$z'_{i,j} = z_{i,j} + j{\cdot}\Delta d. \tag{4}$$

where $z_{i,j}$ is the height value captured by the LT9011 at the ith position in the jth section, and $z'_{i,j}$ is the value after misalignment correction. When the section length was set as 1.1 mm with a sampling spacing of 2 µm, and the external positioning interval was set as 1 mm, there was an overlapping of 0.1 mm with 50 sampling points between neighboring sections.

The least-squares principle can be applied to determine the value of Δd. The optimal Δd should minimize the residual sum of squares (RSS) of the deviation between the neighboring overlaps:

$$\begin{aligned} RSS &= \sum_{j=0}^{m-1}\sum_{i=0}^{n}\left(z'_{i+(n-N),j} - z'_{i,j+1}\right)^2; \\ &= \sum_{j=0}^{m-1}\sum_{i=0}^{n}\left[z_{i+(n-N),j} + j{\cdot}\Delta d - z_{i,j+1} - (j+1)\Delta d\right]^2; \\ &= \sum_{j=0}^{m-1}\sum_{i=0}^{n}\left[z_{i+(n-N),j} - z_{i,j+1} - \Delta d\right]^2. \end{aligned} \tag{5}$$

where m, n and N represent the number of sections, the number of data points in each section and the number of the data points in each overlap. In order to obtain the minimum value of RSS, Δd should comply with the following condition:

$$\frac{\partial RSS}{\partial \Delta d} = 0. \tag{6}$$

With Equation (5) taken into Equation (6):

$$-2\sum_{j=0}^{m-1}\sum_{i=0}^{N}(z_{i+(n-N),j}-z_{i,j+1}-\Delta d)=0. \tag{7}$$

$$\Delta d=[\sum_{j=0}^{m-1}\sum_{i=0}^{N}(z_{i+(n-N),j}-z_{i,j+1})]/[N/(m-1)]. \tag{8}$$

4.3. Profile Restoration

Using Equations (2) and (6), linear misalignment can be well compensated. However, misalignment could be eliminated only when the linear guide had perfect straightness and repeatability. In practical tests, further compensation on the residual mismatch was still needed. Figure 7 shows the concept of compensating the residual mismatch, demonstrated by simulation data. The residual mismatches were compensated by adjusting every alternate data section. Assuming k is an odd number, the mismatches between the kth, $(k-1)$th and $(k \pm 1)$th sections are

$$\begin{cases}\Delta d_k=\frac{1}{N}\sum\limits_{i=0}^{N}z'_{i+(n-N),k-1}-z'_{i,k};\\ \Delta d_{k+1}=\frac{1}{N}\sum\limits_{i=0}^{N}z'_{i,k+1}-z'_{i+(n-N),k}.\end{cases} \tag{9}$$

Then, the further corrected height values are

$$z''_k=z'_k+\Delta d_k+\frac{i}{N}(\Delta d_{k+1}-\Delta d_k). \tag{10}$$

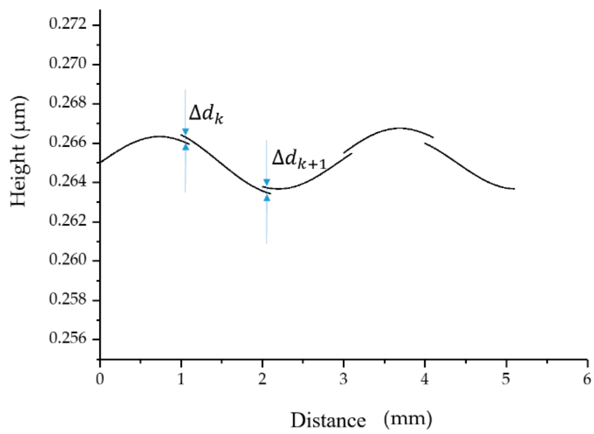

Figure 7. Compensation of residual mismatch.

Considering the redundant data in the overlapping area, in each adjusted section $\{z''_k\}$, the first N data points and the last N data points were removed to connect with the neighboring sections.

4.4. Dual-Scan Positioning Control for Surface Profiling

In the above sections, development of enabling technologies for surface profiling was discussed. As a summary, in this section the algorithm of dual-scan positioning control and surface reconstruction is presented.

In practical measurements, if the surface is relatively flat, the system will scan the surface without vertical positioning control. Misalignment between the internal and external positioning was corrected, as discussed in Section 4.2, and residual mismatch was eliminated as discussed in Section 4.3.

For free-form surface measurements, the system followed the process shown in Figure 8.

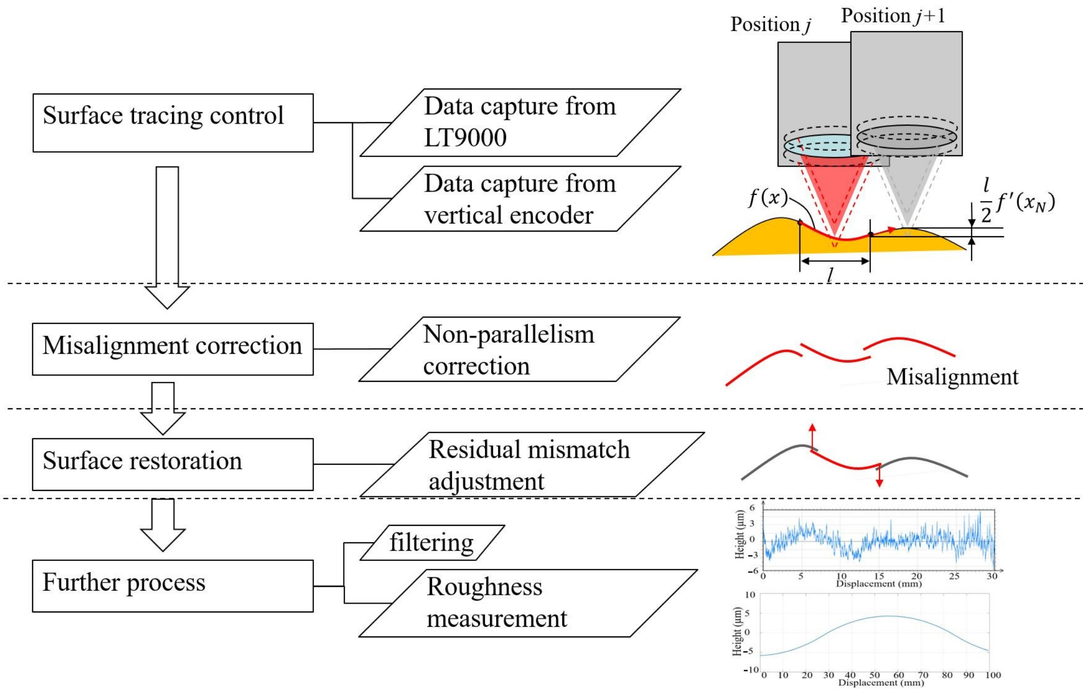

Figure 8. Surface measurement workflow.

With the surface tracing algorithm discussed in Section 4.1, the system was able to capture the surface data by combining the height information captured by LT9011 and the vertical positioner. However, since the data captured in each section were from the internal scan of the LT9011, misalignment between the internal scan and external lateral positioning was not considered.

With the misalignment correction algorithm discussed in Section 4.2, the non-parallelism between the moving axes of internal scan and external lateral positioning can be compensated. After this misalignment correction, the profile may still show mismatches between neighboring sections. This mainly is due to the vertical positioning error and straightness of the lateral movement.

With the profile restoration algorithm discussed in Section 4.3, the mismatches between neighboring sections can be compensated by adjusting data sections with even sequence numbers.

5. Experimental Verification

Experiments were conducted to verify the measurement performance of the proposed dual-scan scanning method. Because temperature-induced deformation of the measurement modules may affect measurement accuracy [28], the measurement tests were performed in an air-conditioned workshop, with temperature controlled at 20 ± 2 °C. The reference systems were also working in a laboratory with the temperature controlled at 20 ± 1 °C. In order to minimize the influence of temperature variation, the data capture processes were completed within 3 min.

An area of 1 mm × 1 mm on an additive manufacturing sample was scanned to verify the areal measurement method as discussed in Section 3. A line scan of 25 mm was conducted to verify the long-travel surface tracing strategy discussed in Section 4.

5.1. Robotic Vibration Test

Since the proposed systems were portable and reconfigurable, the proposed methodology has the potential to be utilized for in situ measurement [29]. Figure 9 shows the robotic application. Vibration tests were conducted on a collaborative robot (UR5, Universal Robots, Odense, Denmark) to address the concern of measurement stability. The measurements were conducted at five different timings and repeated fifty times on the same spot at each timing. The test results (mean ± st. dev) are presented in Table 2. It can be concluded that robotic vibration in standby mode has minimum effects for roughness measurement on the micron to sub-micron level.

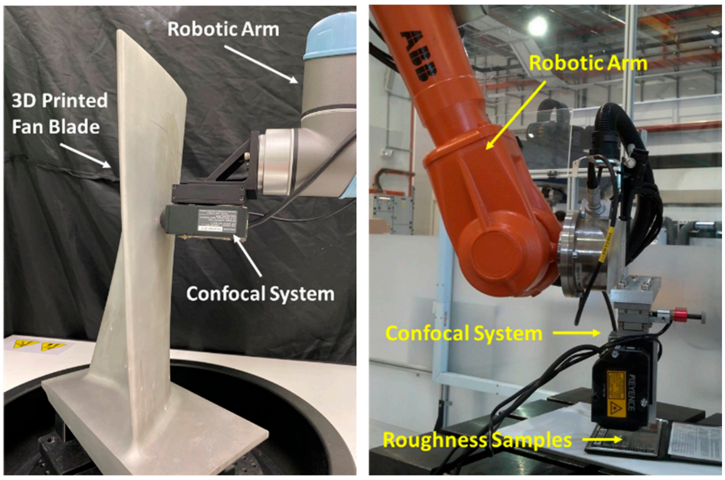

Figure 9. Robotic setup for in situ measurement [25].

Table 2. Measurement results of robotic system vibration.

Timing No.	1	2	3	4	5
Test Result (μm)	63.38 ± 0.02	63.33 ± 0.02	63.30 ± 0.01	63.13 ± 0.02	62.62 ± 0.03

5.2. Area Scan

An external positioner was installed with the moving axis perpendicular to the internal scan of the laser confocal sensor LT9011. The system was introduced in Section 3. As a representative surface with irregular patterns, an additive manufacturing (AM) sample was selected for measurement. A coherence scanning microscope (Talysurf CCI HD, AMETEK Inc., Berwyn, PA, USA) and a spinning-disk confocal microscope (Smartproof 5, Carl Zeiss AG, Oberkochen, Germany) were used as the reference systems for the comparison study. The surface topography of the AM sample measured by different instruments is shown in Figure 10. It can be observed that the measurement results showed consistent surface patterns.

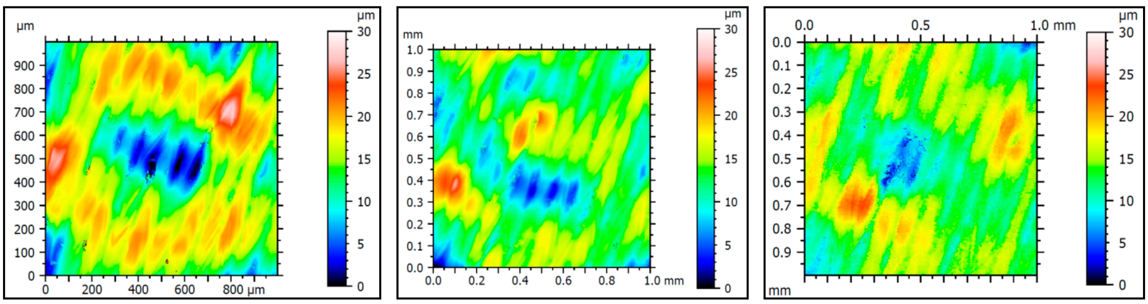

(**a**) (**b**) (**c**)

Figure 10. Surface topography measurement of an additive manufacturing (AM) sample: (**a**) by CCI; (**b**) by Smartproof 5; (**c**) by the proposed system.

For quantitative evaluation, height parameters Sa, Sq and S10z, statistical parameters Ssk and Sku, and surface isotropy parameters Str and Std were employed to evaluate the measurement performance. Comparison results are shown in Table 3, with the standard deviation of five repeats for each measurement.

Table 3. Measurement results of area scans.

	Taylor Hobson CCI	Carl Zeiss Smartproof 5	Proposed System
Sa **(μm)**	2.50 ± 0.10	2.42 ± 0.13	2.41 ± 0.12
Sq **(μm)**	3.26 ± 0.16	3.09 ± 0.19	3.04 ± 0.17
S10z **(μm)**	24.95 ± 0.16	23.02 ± 0.27	22.09 ± 0.17
Ssk	−0.18 ± 0.01	−0.14 ± 0.01	−0.17 ± 0.02
Sku	3.40 ± 0.04	3.58 ± 0.04	3.37 ± 0.08
Str	0.19 ± 0.01	0.21 ± 0.00	0.18 ± 0.02
Std **(°)**	69.97 ± 0.14	71.04 ± 0.10	70.58 ± 0.13

5.3. Long-Travel Line Scan

A free-form sample was fabricated to verify the long-travel measurement capability of the proposed dual-scan surface tracing system. The system setup is shown in Figure 5a. Areas with different roughness were intentionally made on the sample surface. The surface roughness measurement results are shown in Table 4, with a standard deviation of five repeats for each measurement. A stylus profilometer (Talysurf PGI 800, AMETEK Inc., Berwyn, PA, USA) was used as the reference system.

Table 4. Long-travel roughness measurement results.

		PGI 800	Proposed System	Absolute Error	Relative Error
Zone 1	***Ra*** (μm)	0.56 ± 0.01	0.58 ± 0.02	0.02	3.6%
	Rq (μm)	0.69 ± 0.01	0.72 ± 0.03	0.03	4.3%
Zone 2	***Ra*** (μm)	0.93 ± 0.02	0.97 ± 0.05	0.04	4.3%
	Rq (μm)	1.14 ± 0.02	1.19 ± 0.07	0.05	4.4%
Zone 3	***Ra*** (μm)	1.36 ± 0.01	1.42 ± 0.04	0.06	4.4%
	Rq (μm)	1.70 ± 0.01	1.78 ± 0.06	0.08	4.7%

6. Conclusions and Future Work

In this paper, surface texture measurement methodology based on a dual-scan scanning mechanism has been proposed for surface texture measurement. The motivation for this study was to address the challenges of measuring surfaces with geometric complexity and irregular surface pattern.

By setting the internal and external scanning in perpendicular directions, the system was able to perform area measurements. Areal parameters to evaluate the surface quality were obtained, including height parameters *Sa*, *Sq* and *S10z*, statistic parameters *Ssk* and *Sku*, and surface isotropy parameters *Str* and *Std*.

By setting the internal and external scanning in parallel directions, the system was able to perform line measurements over long travels. A misalignment compensation algorithm was developed to reduce the measurement error due to non-parallelism and straightness errors.

Commercial 3D microscopes (Talysurf CCI and Zeiss Smartproof 5) and a tactile stylus profilometer (Talysurf PGI 800) were employed to evaluate the measurement performance of the proposed methodology. For area measurement in a range of 1 mm by 1 mm, and for line measurement in a scan length up to 100 mm, experimental results showed that the proposed systems were able to achieve comparable accuracy with the commercial systems.

Future work will focus on further analyzing the effects of robotic vibration and environmental temperature variation and on developing advanced noise filtering and error compensation algorithms. In addition, the developed in situ measuring system will be fully integrated into a robotic polishing cell to conduct in situ measurements as a tool of quality verification.

Author Contributions: Conceptualization, F.C. and S.F.; methodology, F.C. and S.F.; software, S.F.; validation, S.F.; formal analysis, S.F.; investigation, S.F.; resources, F.C. and Z.C.; data curation, S.F.; writing—original draft preparation, F.C.; writing—review and editing, F.C. and S.F.; visualization, F.C. and S.F.; supervision, F.C.; project administration, F.C. and S.F.; funding acquisition, Z.C. All authors have read and agreed to the published version of the manuscript.

Funding: This work was funded by the National Natural Science Foundation of China (Grant No. 51775075, 51935004).

Conflicts of Interest: The authors declare no conflict of interest.

References

1. Davim, J.P. *Surface Integrity in Machining*; Springer: London, UK, 2010.
2. Whitehouse, D. *Surfaces and Their Measurement*; Butterworth-Heinemann: London, UK, 2004.
3. Fay, M.F.; Badami, V.G.; De Lega, X.C. Characterizing additive manufacturing parts using coherence scanning interferometry. In Proceedings of the ASPE Spring Topical Meeting on Dimensional Accuracy and Surface Finish in Additive Manufacturing, Berkely, CA, USA, 13–16 April 2014; pp. 135–138.
4. Triantaphyllou, A.; Giusca, C.L.; Macaulay, G.D.; Leach, R.K.; Milne, K.A. Surface texture measurement for additive manufacture. *Surf. Topogr. Metrol. Prop.* **2015**, *3*, 024002. [CrossRef]
5. Whitehouse, D.J. Surface metrology. *Meas. Sci. Technol.* **1997**, *8*, 955–972. [CrossRef]
6. Bradley, C. Automated Surface Roughness Measurement. *Int. J. Adv. Manuf. Technol.* **2000**, *16*, 668–674. [CrossRef]
7. Whitehouse, D. A new look at surface metrology. *Wear* **2009**, *266*, 560–565. [CrossRef]
8. Cheng, F.; Fu, S.W.; Leong, Y.S. Research on optical measurement for additive manufacturing surfaces. In Proceedings of the SPIE International Conference on Optical and Photonics Engineering, Chengdu, China, 26–30 September 2016.
9. British Standards Institution. *BS EN ISO 4287 Profile Method—Terms, Definitions and Surface Texture Parameters*; BSI: London, UK, 1998.
10. Sandoz, P.; Tribillon, G.; Gharbi, T.; Devillers, R. Roughness measurement by confocal microscopy for brightness characterization and surface waviness visibility evaluation. *Wear* **1996**, *201*, 186–192. [CrossRef]
11. Paddock, S.W. *Confocal Microscopy*; Humana Press: Totowa, NJ, USA, 1998.
12. Rishikesan, V.; Samuel, G.L. Evaluation of Surface Profile Parameters of a Machined Surface Using Confocal Displacement Sensor. *Procedia Mater. Sci.* **2014**, *5*, 1385–1391. [CrossRef]
13. Yoshizawa, T. *Handbook of Optical Metrology: Principles and Applications*; CRC Press: Boca Raton, FL, USA, 2009.
14. Hocken, R.J.; Chakraborty, N.; Brown, C. Optical Metrology of Surfaces. *CIRP Ann. Manuf. Technol.* **2005**, *54*, 169–183. [CrossRef]
15. Viotti, M.R.; Albertazzi, A.; Fantin, A.V.; Pont, A.D. Comparison between a white-light interferometer and a tactile formtester for the measurement of long inner cylindrical surfaces. *Opt. Lasers Eng.* **2008**, *46*, 396–403. [CrossRef]
16. Danzl, R.; Helmli, F.; Scherer, S. Focus variation—A robust technology for high resolution optical 3D surface metrology. *J. Mech. Eng.* **2011**, *57*, 245–256. [CrossRef]
17. Newton, L.; Senin, N.; Gomez, C.; Danzl, R.; Helmli, F.; Blunt, L.; Leach, R. Areal topography measurement of metal additive surfaces using focus variation microscopy. *Addit. Manuf.* **2019**, *25*, 365–389. [CrossRef]
18. British Standards Institution. *BS EN ISO 25178-2 Terms, Definitions and Surface Texture Parameters*; BSI: London, UK, 2012.
19. Leach, R. *Characterisation of Areal Surface Texture*; Springer: Berlin/Heidelberg, Germany, 2013; p. 17.
20. Chen, L.C. Full-field chromatic confocal surface profilometry employing digital micromirror device correspondence for minimizing lateral cross talks. *Opt. Eng.* **2012**, *51*, 081507. [CrossRef]
21. Blateyron, F. *Chromatic Confocal Microscopy. Optical Measurement of Surface Topography*; Springer: Berlin/Heidelberg, Germany, 2011; pp. 71–106.
22. British Standards Institution. *BS EN ISO 16610-21 Linear Profile Filters: Gaussian Filters*; BSI: London, UK, 2012.
23. Fu, S.; Cheng, F.; Tjahjowidodo, T. Surface Topography Measurement of Mirror-Finished Surfaces Using Fringe-Patterned Illumination. *Metals* **2020**, *10*, 69. [CrossRef]
24. Fuh, Y.-K.; Fan, J.R.; Huang, C.Y.; Jang, S.C. In-process surface roughness measurement of bulk metallic glass using an adaptive optics system for aberration correction. *Measurement* **2013**, *46*, 4200–4205. [CrossRef]

25. Fu, S.; Cheng, F.; Tjahjowidodo, T.; Zhou, Y.; Butler, D. A Non-Contact Measuring System for In-Situ Surface Characterization Based on Laser Confocal Microscopy. *Sensors* **2018**, *18*, 2657. [CrossRef] [PubMed]
26. Fu, S.; Cheng, F.; Tjahjowidodo, T.; Liu, M. Development of an Image Grating Sensor for Position Measurement. *Sensors* **2019**, *19*, 4986. [CrossRef] [PubMed]
27. Fu, S.; Cheng, F.; Tjahjowidodo, T.; Liu, M. Image grating: A novel technology for position measurement. In Proceedings of the Seventh International Conference on Optical and Photonic Engineering, Phuket, Thailand, 16–20 July 2019.
28. Grochalski, K.; Wieczorowski, M.; Pawlus, P.; H'Roura, J. Thermal Sources of Errors in Surface Texture Imaging. *Materials* **2020**, *13*, 2337. [CrossRef] [PubMed]
29. Fu, S.; Kor, W.S.; Cheng, F.; Seah, L.K. In-situ measurement of surface roughness using chromatic confocal sensor. *Procedia CIRP* **2020**, *94*, 780–784. [CrossRef]

Publisher's Note: MDPI stays neutral with regard to jurisdictional claims in published maps and institutional affiliations.